# Reproducibility of Quantitative Cerebral T2 Relaxometry, Diffusion Tensor Imaging, and 1H Magnetic Resonance Spectroscopy at 3.0 Tesla

**J. F. Jansen[1], M. E. Kooi[1], A. G. Kessels[2], K. Nicolay[3], and W. H. Backes[1]**

[1]Department of Radiology, Maastricht University Hospital, Maastricht, Netherlands, [2]Department of Clinical Epidemiology and Medical Technology Assessment, Maastricht University Hospital, Maastricht, Netherlands, [3]Biomedical NMR, Department of Biomedical Engineering, Eindhoven University of Technology, Eindhoven, Netherlands

## Introduction

Reproducibility is defined as the extent to which repeated measurements on the same subject are in agreement [1]. It is important to study the reproducibility of quantitative MR methods, as individual changes associated with a certain pathology or advancing age can only be detected when the deviation from normal values are larger than the reproducibility of that particular measurement. It is also essential to know the reproducibility in order to determine whether measured tissue values can be classified as normal or abnormal. We set out to assess the reproducibility of T2 relaxometry, diffusion tensor Imaging (DTI), and chemical shift imaging (CSI) of the brain on a clinical 3.0 T MR system.

## Material and Methods

Ten young healthy adults were imaged on two separate days with a 3.0-T whole-body unit (Philips Achieva). Each session consisted of an imaging part using an 8 channel SENSE head coil and a spectroscopy part using a T/R head coil. For T2 quantification a 3D TSE-Dual was performed, using: TR 2500 ms, $TE_1$ 10 ms, $TE_2$ 110 ms, matrix 256x256x100, FOV 256x256x200 $mm^3$, 2.0 mm adjacent coronal slices, SENSE factor 1.5 left-right. DTI images were obtained with a EPI-SE sequence, using: b-values 0 and 800 $s/mm^2$, TR 6600 ms, TE 62 ms, 15 gradient directions for diffusion sensitization (gradient overplus on), matrix 128x128x66, FOV 256x256x132 $mm^3$, 2 mm adjacent transverse slices, SENSE factor 2.5 anterior-posterior. Two slices were selected for spectroscopic imaging, one accommodated in the temporal and one in the frontal lobe, respectively, using: 20×20 voxels per slice, FOV 256×256 $mm^2$, slice thickness 20 mm, TR 2.0 s, TE 30 ms, a nominal voxel size of 3.3 ml, echo acquisition half echo. Localization and water suppression was achieved with PRESS and CHESS, respectively. The T2 was calculated (in ms) on a voxel-by-voxel basis using the signal intensities of the images obtained at the two echo times (Matlab). From these values also a percentile volume cerebrospinal fluid (CSF) map was calculated. The ADC (in $10^{-6}$ $mm^2/s$) and FA (in %) maps were calculated using the diffusion software available on the MRI scanner. The T2-, CSF-, FA- and ADC-maps were spatially normalized to Talairach space, to facilitated analysis of brain regions with masks. Absolute metabolite quantification was performed using LCModel and the calibration strategy was based on the principle of reciprocity [2]. Concentrations were corrected for cerebrospinal fluid (CSF) contribution, using the CSF-map. The metabolite estimations for choline (Cho), creatine (Cr), myoinositol (mI) and n-acetyl-aspartate (NAA) were analyzed. Metabolite estimates were excluded from reproducibility analysis, if the Cramer-Rao minimum variance exceeded the 20% range. Furthermore, at least 5 volunteers should have reliable spectra in a voxel. Statistical analysis of the T2-, ADC-, and FA-maps was performed in the frontal and temporal lobe, and the entire cerebrum. Descriptive statistics were derived on a voxel-by-voxel basis, and then summarized per region by calculating the median. The coefficient of variation (CV, derived as the mean within-subjects standard deviation ($SD_{ws}$) divided by the mean value for all subjects [3]), the repeatability coefficient (RC = 1.95 * √2 * SDws [3]) and the intraclass correlation coefficient (ICC = $SD_{bs}^2$ / ($SD_{bs}^2$ + $SD_{ws}^2$), where $SD_{bs}$ represents between-subjects standard deviation [1]) were chosen as measures of precision. T2-, ADC-, and FA-maps were smoothed using a Gaussian kernel with FWHM of 6 mm.

| Technique | Measured quantity | Cerebral region | Average median session 1* | Average median session 2* | CV (%) | RC* | ICC |
|---|---|---|---|---|---|---|---|
| TSE-Dual | T2 (ms) | Frontal | 79.0 | 77.5 | 3.9 | 8.5 | 0.59 |
| | | Temporal | 78.6 | 80.2 | 4.7 | 10.4 | 0.61 |
| | | Cerebrum | 78.4 | 78.3 | 4.3 | 9.5 | 0.56 |
| DTI | ADC ($10^{-6}$ $mm^2/s$) | Frontal | 784 | 781 | 3.2 | 69 | 0.70 |
| | | Temporal | 800 | 804 | 3.5 | 78 | 0.75 |
| | | Cerebrum | 786 | 788 | 3.4 | 74 | 0.73 |
| | FA (%) | Frontal | 38.3 | 39.0 | 6.4 | 6.9 | 0.75 |
| | | Temporal | 35.2 | 35.7 | 6.7 | 6.8 | 0.86 |
| | | Cerebrum | 37.4 | 37.9 | 6.5 | 6.7 | 0.80 |
| CSI (mmol per kg wet weight) | NAA | Frontal | 11.5 | 11.0 | 13.8 | 4.1 | 0.28 |
| | | Temporal | 8.8 | 9.4 | 16.1 | 4.2 | 0.19 |
| | Cr | Frontal | 7.0 | 6.7 | 14.3 | 2.8 | 0.28 |
| | | Temporal | 8.0 | 8.3 | 18.9 | 3.1 | 0.04 |
| | Cho | Frontal | 1.9 | 1.9 | 13.8 | 0.8 | 0.26 |
| | | Temporal | 1.6 | 1.6 | 27.3 | 1.1 | 0.00 |
| | mI | Frontal | 3.9 | 3.7 | 17.2 | 1.9 | 0.18 |
| | | Temporal | 4.3 | 4.1 | 30.4 | 3.8 | 0.18 |

**Table 1** Descriptive statistics of reproducibility measures, derived on a voxel-wise basis, and averaged per region. CV indicates coefficient of variation, RC, repeatability coefficient, ICC, intraclass correlation coefficient. *in units of the MR measured quantity.

## Results

Table 1 displays the reproducibility characteristics for each quantitative measure. For all measured quantities, the obtained values lie within the expected range as measured in previous studies at 3.0T [4,5]. In figure 1A-C, the areas that display high CV values for the T2, ADC and FA measures are projected on a transverse T1-weighted slice. Several regions display less favorable reproducibility characteristics (expressed by high CV values). Most of these regions (indicated with yellow arrows in figure 1B) display a large variability in CSF content. The areas (indicated with red arrows in figure 1B) that display less favorable reproducibility characteristics, which are not related to different CSF contributions, are part of the basal ganglia. In figure 1D and 1E the CV per voxel of CSI is visualized for the temporal and frontal slice, respectively. Voxels with less favorable reproducibility characteristics, expressed either by high CV values, or low quality characteristics (indicated by white crosses), for both slices were found lateral, close to the skull. Results for T2 relaxometry, DTI as well as $^1$H-MRS were similar to or better than previously reported reproducibility measures from 1.5 T [6,7].

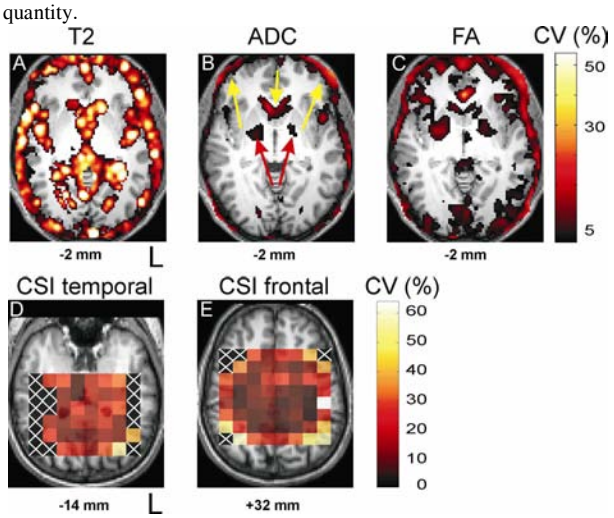


**Figure 1** Regions with unfavorable reproducibility characteristics, expressed using their CV. **(A)** T2, **(B)** ADC, **(C)** FA, **(D)** NAA temporal, and **(E)** NAA frontal slice, respectively. Voxels that did not fulfill the quality control criteria are marked with white crosses. Slice positions are given in approximate stereotaxic Talairach z-coordinates.

## Discussion

For the CSI experiment, the frontal lobe displayed far better characteristics than the temporal lobe, as this lobe is close to the tissue-bone interface and air cavities near the skull base (increased B0 inhomogeneity). The voxels with large CV values for the T2-map (figure 1A) all have (partial) contribution from the CSF. The brain regions close to the CSF spaces (i.e. ventricles and pericortex) display large CV values due to the highly variable size of CSF containing compartments throughout the volunteer population. A reason for the fact that the part of the basal ganglia also displays high CV values, might be explained by susceptibility artifacts induced by the high levels of iron within the basal ganglia [8]. Despite increased magnetic field inhomogeneities within the tissue at 3.0 T, the reproducibility of quantitative brain MRI at 3.0 T is better than or at least comparable to the reproducibility at 1.5 T.

## References

[1] Tofts P, qMRI of the brain 2003. [2] Soher, BJ. Magn Reson Med 1996; 35:356-363. [3] Bland JM, et al Lancet 1986; 1: 307-310. [4] Stanisz GJ, et al. Magn Reson Med 2005; 54:507-512. [5] Huisman TA, et al. Eur Radiol 2006; 16:1651-1658. [6] Larsson HB, et al. Magn Reson Imaging 1992; 10:579-584. [7] Pfefferbaum A, et al. J Magn Reson Imaging 2003; 18:427-433. [8] Drayer, B. AJNR 1986; 147:103-110.